Chapter 15

Carbon Nanotubes as Suitable Interface for Improving Neural Recordings

Gemma Gabriel, Xavi Illa, Anton Guimera, Beatriz Rebollo, Javier Hernández-Ferrer, Iñigo Martin-Fernandez, Mª Teresa Martínez, Philippe Godignon, Maria V. Sanchez-Vives and Rosa Villa

Additional information is available at the end of the chapter

http://dx.doi.org/10.5772/52174

1. Introduction

In the last decades, system neuroscientists around the world have dedicated their research to understand how neuronal networks work and how they malfunction in various diseases. Furthermore in the last years we have seen a progressively increased interaction of brain networks with external devices either for the use of brain computer interfaces or through the currently extended brain stimulation (e.g. transcranial magnetic stimulation) for therapy. Both techniques have evidenced even more the need for a better understanding of neuronal networks. These studies have resulted in the development of different strategies to understand the ongoing neuronal activity, such as fluorescence microscopy for genetic labelling and optogenetic techniques, imaging techniques, or the recording/stimulation with increasingly large numbers of electrodes in the whole brain or in both cell cultured neurons and slice preparations. It is in these last two areas where the technology developed on microelectrode arrays, commonly called multi-electrode arrays (MEAs), has become important over other technologies [1–3].

MEA devices are formed by a large number of microelectrodes arrayed on substrates with small geometry size in order to excite or register a group of neurons selectively and efficiently. There are several applications where MEA devices are crucial for nerve recording and stimulation. Some of these are limb prostheses for spinal cord injuy; bladder prostheses, cochlear and brain-stem auditory prostheses, retinal and cortical visual prostheses, cortical

recordings, vagus nerve stimulation for epilepsy and depression, deep brain stimulation, Parkinson's disease, epilepsy, dystonia and depression. In such areas, advances on microfabrication technology have given rise to a great success in the neural interfaces field.

A MEA can be used to perform electrophysiological experiments on tissue slices or dissociated cell cultures. With acute tissue slices, the connections between the cells within the tissue slices prior to extraction and plating are more or less preserved, while the intercellular connections in dissociated cultures are destroyed prior to plating. With dissociated neuronal cultures, the neurons spontaneously form networks.

Related to the work presented here, brain slices provide more information of a realistic model where the brain architecture is maintained. Furthermore, one of our aims is to carry out developments that are as well usable for in vivo interfacing, both in acute and chronic situations. However, these emerging technologies do still face tremendous challenges mainly related with long-term experiments. Electrodes are metallic conductors (the most common ones Pt, Pt alloys, Ir oxide and TiN), however, for chronic stimulation and recording they present some drawbacks as, for example, for obtaining and maintaining good recordings. This is a consequence of the difficulty to assure both good electrochemical electrode response and good contact between the electrode and the tissue. This is mainly a consequence of the electrode material and the planarity of the substrate used to fabricate the MEAs. Recently, different technologies have been proposed to overcome these limitations such us electrochemical deposition of conductive polymers [4–6] and the use of carbon nanotube (CNT) coatings which has been extensively demonstrated to improve neuronal recordings [7–11]. Also it can be found in the literature a broad type of materials that can be deposited over the electrode to enhance the response of a recording electrodes. The most well-known are stain-less steel, tungsten, platinum, platinum-iridium alloys, iridium oxide, titanium nitride or poly(etylenedioxythiophene (PEDOT).

CNTs are high aspect ratio, exceptionally strong, tough, and show desirable chemical and electrical properties [12, 13]. Hence, they are attractive for interfacing with neural systems to develop biocompatible, durable and robust neuroprosthetic devices turning into an excellent candidate for the improvement of neural interfaces [14,15]. CNTs can be grown or assembled on a great variety of surfaces and can give rise to electrodes with different morphologies.

Based in the great experience of our research group, the aim of this work is to explain the different electrode modification methods we have developed. We have demonstrated the modification of the surface from multielectrode devices by drop casting Single Walled Carbon Nanotubes (SWNTs) [16, 17] and by selectively synthesizing arrays of Multi Walled Carbon Nanotubes (MWNTs) by chemical vapour deposition (CVD) [18,19]. The drop casting of SWNTs was demonstrated to be an easy method to perform electrode modification technique that results in a high purity CNT interface with spaghetti like morphology. The area of the electrode is one of the most important limitations of this technique as it cannot be implemented in electrodes higher than 100 μm [17]. Another option is the direct growth of MWCNTs on the metal substrate that results in a more robust electrode along the application lifetime. With this method, the electrode dimension is not a limitation. Moreover, fully

http://dx.doi.org/10.5772/52174

biocompatible materials can be used during the fabrication process as we demonstrated platinum catalysts for the growth of CNTs [19]. In conclusion, we stated that the vertically aligned CNT array morphology has advantages regarding the voltammetric measurements over the drop casted one.

However, in our first attempts the impedance characteristics of the obtained MWNTs showed a lack of improvement compared to the bare electrode. This was mainly attributed to the presence of amorphous carbon covering the carbon nanotubes that finally inhibit the electron exchange. This issue was solved once the technological process for the integration of pure and dense arrays of vertically aligned MWNTs by using platinum catalysts on the MEAs was found [20]. This method, which is compatible with the wafer scale fabrication technology, is based on standard microelectronic fabrication processes, and only involves the use of bio-compatible materials. The wafer scale compatibility of the process is very important in order to ensure the reproducibility between devices.

In this work these two types of CNT-modified electrodes will be compared to the bare platinum electrode. In particular, arrays of 40 μm in diameter bare platinum electrodes have been used for all the experiments. The size of the electrodes has a strong influence on the impedance value, as the impedance increases with decreasing the electrode area. Thus, the 40 μm bare platinum electrodes used here have very high impedance values that make them useless for the aim of this work. Then, in order to compare the modified CNT-based microelectrodes with useful metallic based electrodes, they were alternatively prepared with electrodeposited black platinum. Electrochemical deposition of black platinum is a common approach for the modification of the surface of microelectrodes in order to reduce their interface impedance by increasing the surface roughness [21,22]. Actually, their electrode-electrolyte impedance values are 10-fold below the bare platinum electrodes.

Besides the contact problems which can be overcome by using CNT or black platinum coatings, the use of silicon or pyrex-based multisite substrates has another main limitation related to the lack of adaptability to biological tissues. This is another cause for obtaining bad measurements due to bad contact that if wanted to be improved in-situ may dramatically damage the biological tissue. The use of the technologies employed in microelectronic fabrication processes along with the development of new polymers have paved the way for the fabrication of polymer-based flexible microprobes with integrated MEAs. In addition, their simple fabrication process and biocompatibility have given to polymeric substrates even more relevance [23,24].

In particular, flexible neural microprobes have been mainly fabricated in polyimide wherein a metal layer is used for the recording sites [25–27]. Other materials like parylene [23,28], benzocyclobutene (BCB) [21] and SU-8 [29,30] have been also employed to fabricate flexible microprobes, demonstrating the interest in this field. In this work, SU-8 has been chosen due to the expertise of our group and its low-cost and versatile fabrication process.

Dealing with the surface electrode improvements, the use of flexible materials implies the use of new strategies as the above described surface modifications with carbon nanotubes are not compatible with these polymeric materials. Basically, the CNTs growth method can

not be used due to the high temperatures required, while the drop casting SWNTs method can not be applied to flexible MEAs due to the fragility of these substrates. On the contrary, regarding the black platinum electrodeposition, the use of flexible substrates does not suppose a problem.

However, an alternative method to use CNTs for the modification of the microelectrodes on polymeric substrates has been lately described by using a CNTs/polypyrrole electrodeposition [31–34]. With this method, SWCNTs/polypyrrole (Ppy) films can be electrochemically grown over the electrodes on the transparent and flexible polymeric substrates [28,29,35]. The presence of SWCNTs during a slow polymerization of Ppy results in a high rough surface electrode because the polymeric coating in course entraps the SWCNTs.

In this work, validation of the CNT integrated MEAs is performed by comparing them to non-modified metal electrodes using two strategies. Firstly, the electrode-electrolyte interface has been characterized by impedance spectroscopy and by cyclic voltammetry to compare their electrode-electrolyte interfaces as along with ex-situ techniques for film characterization. Secondly, the spontaneous activity from slices of cerebral cortex has been recorded before and after the blockade inhibition in order to demonstrate its feasibility. The obtained results demonstrate the huge potential of such nanostructured materials to build an interface between the neural system and the state of the art nanoelectronics.

2. Materials and methods

2.1. Microelectrode Arrays Fabrication

2.1.1. MEA fabrication

The MEA chips are formed of 16 platinum electrodes that are connected to metal pads located on the sides of the chip not to interfere on the liquid based testing. The electrodes may be circle or square shaped with their diameter or side being 40 or 300 μm. However, all the electrochemical characterizations and the experimental section were conducted with the round 40 μm electrodes.

The electrodes are fabricated similarly as it is described in [16,19] as shown in Figure 1. This figure describes the electrode fabrication from 1a to 1d, and also describes the post process modification of carbon nanotube growth from 1e to 1h. It has been represented in a single figure because it is really implemented as a single process. The starting point is a 4 inch Si wafer (Fig. 1a). First, a 1.5 μm thick SiO2 layer is deposited by plasma enhanced (PECVD) (Fig. 1b). Then, the electrodes, the contact pads and the strips connecting them are patterned after a photolitography, a Ti/Pt deposition (30/150 nm) and a lift-off process (Fig. 1c). Next, the wafer is passivated by a SiO2 and Si3N4 bi-layer (400/700 nm) that is deposited by PECVD and windows are only opened at the electrodes and the connection pads by a second photolithography and a reactive ion etching process (Fig. 1d).

http://dx.doi.org/10.5772/52174

Once the wafer is fabricated the MEAs are encapsulated before the electrodes are electrochemically characterised. First, the wafer is diced by a dicing saw. Then, the MEAs are glued to previously fabricated Printed Circuit Board (PCB), the connection pads are wire-bonded and the wires are protected with an epoxy based resist. Last, a ring lid is glued to the PCB prior to the electrode characterization so that the solution is confined to it during the experiments. A picture of the encapsulated final device is shown in Figure 3A.

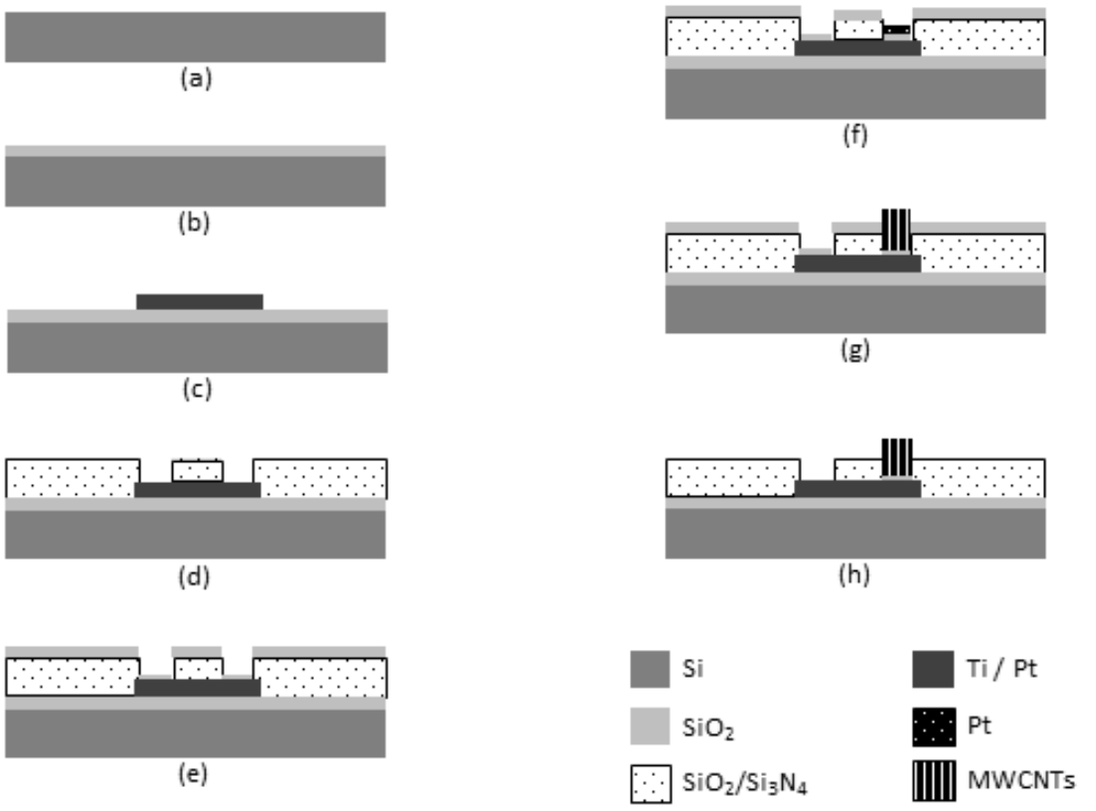

Figure 1. Schematic of the main steps of the fabrication of the electrodes modified with locally grown MWCNTs: (a) initial Si substrate; (b) deposition of a SiO2 layer; (c) patterning of the Ti-Pt electrodes, strips and connection pads; (d) passivation of the electrodes by a SiO2-Si3N4 bi-layer except for the electrodes and the connection pads; (e) deposition of a 15 nm thick layer of SiO2; (f) selective deposition of a Pt thin layer on the electrodes; (g) synthesis of the MWCNTs; (h) removal of the thin SiO2 layer

2.1.2. Flexible MEA fabrication

In this work, flexible microprobes integrating 16 platinum microelectrodes of 40 μm in diameter have been fabricated using SU-8 negative photoresist (Microchem, USA). The fabrication process has taken advantage of our recent work where SU-8-based microneedles for neural applications have been fabricated [29,30,36,37]. In brief, the fabrication process starts with the oxidation of a 4-inch silicon wafer (Fig. 2a). A 400 nm of SiO_2 will serve as a sacrificial layer for the final release of the SU-8 structures. Then a, a 25 μm thick SU-8 structural

layer is deposited, baked, exposed through a mask where the shape of the microprobe is defined, and developed following the conditions defined by the SU-8 manufacturer (Fig. 2b). Afterwards, 20 nm of titanium and 200 nm of platinum are deposited by e-beam evaporation on top of the SU-8 (Fig. 2c). Subsequently, patterning of the metal layer is performed using standard photolithography steps and wet chemical etching (Fig. 2d).

In order to insulate the metal tracks a second SU-8 layer is processed on top of the wafer (Fig. 2e). This 1 μm thick passivation layer also defines the area of the microelectrodes which was designed to be 40 μm in diameter. Finally the whole wafer was immersed in a HF bath to etch the SiO_2 sacrificial layer, releasing the SU-8 microprobes with integrated MEA (Fig 2f).

To facilitate the use of the fabricated microprobes, they were connected to a printed circuit board (PCB) by means of zero insertion force (ZIF) connectors. For that, the connecting pads of the microprobe where designed to match the specifications of the desired ZIF connector. The use of these connectors to encapsulate the microprobes for both characterization and experimentation purposes provides ready-to-test microprobes, as no additional back-end fabrication process is needed. In Fig. 3b there is an image of an individual SU-8 microprobe where it can be observed the high flexibility that can be obtained with the presented fabrication process.

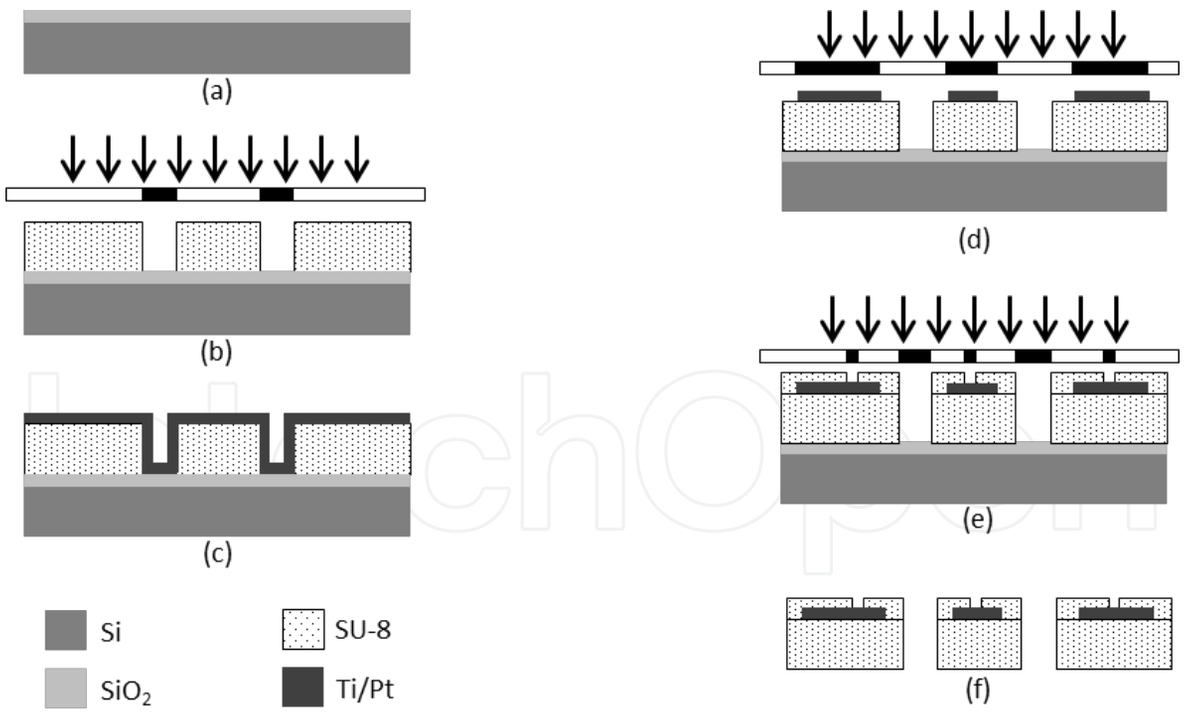

Figure 2. Schematic of the main steps of the fabrication of the electrodes in flexible SU-8 substrate: (a) deposition of a SiO2 layer; (b) deposition and patterning of the 25 μm SU-8 substrate; (c) deposition of the Ti/Pt metal layer; (d) patterning of the Ti-Pt electrodes, strips and connection pads; (e) deposition and patterning except for the electrodes and the connection pads of a 1 μm thick SU-8 layer acting as passivation; (f) etch of the sacrificial layer and release of SU-8 microprobes.

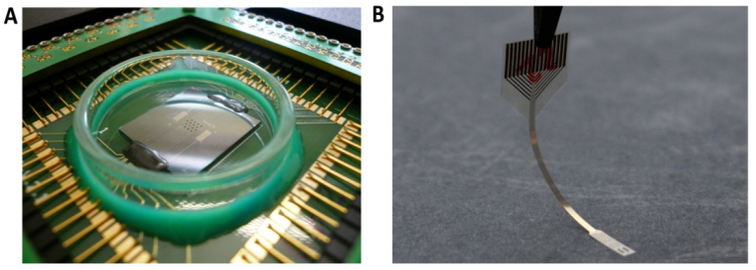

Figure 3. A, picture of standard silicon MEA of 16 electrodes provided with the lid ring and encapsulated to a Printed Circuit Board. B) Flexible SU-8 MEA of 16 electrodes.

2.2. Electrode post-processing strategies

The post-processing strategies are an enhancement of the electrode behaviour focused on the modification of the electrode surface area, so they can be described independently of the substrate of the MEA device. However, it must be taken into account the limitations that present the material substrates of the microprobes used in this work. In this way, the drop casting SWNTs methodology can not be applied to our fabricated flexible SU-8 MEAs due to the fragility of thes 20 μm thick probes. For thicker SU-8 probes this would not suppose a problem. Likewise, the CNTs growth method here described can not be applied to the SU-8 microprobes due to the high temperature requirements that the chemical vapour deposition (CVD) carbon nanotubes growth requires. The other methods can be used alike.

2.2.1. Black platinum electrodeposition

Ti/Pt electrodes on individual devices were electrochemically coated with a porous layer of black platinum to reduce their impedance through a customized process of platinization [38]. Platinization was carried out using a Pt electrode (Radiometer Analytical) in a LC20H Ultrasonic Cleaner (Elma) and involved an initial cleaning of the electrode surface for 3 min in ethanol with 35 kHz ultrasounds. Afterwards, the electrode surfaces were activated in a KCl 0.1M solution until release of H2 was apparent. Thereafter, electroplating was performed for 1 min in a solution containing platinum chloride (Hydrochloric acid 0.1M, 2.3% Platinum (IV) chloride and 0.023% Lead (IV) acetate 99 %. All reagents were analytical grade (Panreac) and used as received. The injected current was of 20mA for 40 μm Ø electrodes. Finally they were introduced again in an ultrasound cleaner, in order to blast off poorly adhered platinum from the electrode surface.

2.2.2. Drop casting SWNTs

High purity Single Walled Carbon Nanotubes (SWNTs) were purchased from Sigma Aldrich. Carbonaceous purity is about 88 % and may contain about 3 to 6 atomic % of carboxylic acid groups due to acidic purification. Thermogravimetric analyses showed a metal content of 6 % wt. Raman spectra revealed a mean diameter of 1.3-1.6 nm and confirmed a low carbonaceous content. For the modification of the Pt microelectrodes with SWNTs, 10

mg of pure SWNTs were dispersed in 10 ml of dimethyl formamide (DMF) under ultrasonic agitation resulting in a 1 mg/ml black suspension [16,17]. Once the Pt electrode was cleared with ethanol, the surface was coated by dropping the suspension of SWNTs in DMF, and dried at 90-100 ºC. Finally, the device was thoroughly rinsed with distilled water and mechanically cleaned to ensure that carbon nanotubes stayed delimited in the electrode area.

2.2.3. MWNTs growth

The integration of the MWCNT arrays can be implemented as a continuation of the described MEA device fabrication in the section 2.1.1, in this way, the CNTs growth is also compatible with large wafer scale fabrication. This facilitates to obtain an homogenous electrical response for the different modified MEAs.

The MWNT growth starts by the deposition of a 15 nm thick SiO2 layer. On the one side, this layer aims to inhibit the diffusion of the catalyst material into the electrode and, on the other side, to increase the roughness of the electrode to enhance the formation of a dense array of CNTs in the subsequent steps (Figure 1e). Afterwards, the catalyst material for the MWCNTs to grow from is selectively patterned on the electrodes by a photolithography, the deposition of a 4 nm thick layer of Pt and a lift-off process (Figure 1f). The MWCNTs are synthesized in a rapid thermal CVD system at 800ºC by H2 and CH4 as the main process gases in a 2 step process. The first step aims at dewetting the Pt layer into a dense array of ~10 nm diameter nanoparticles and, during the second step the MWCNT arrays are made to grow after the flow of the carbon containing gas (CH4 in this case)are made to grow into the chamber (Figure 1g). The last step of the fabrication is the removal of the 15 nm thick SiO2 layer by a HF based solution (Figure 1h).

2.2.4. SWNTs/polypyrrol composite electrodeposition

Sodium monohydrogenophosphate heptahydrate, sodium dihydrogenophosphate monohydrate (puriss. p.a.), sodium dodecylbenzenesulfonate (technical grade), yttrium (99.9%) and graphite powder (≥99.99%) were purchased from Aldrich. Nickel powder (99.9%) was purchased from AlfaAesar (website http://www.alfa.com). Graphite bars were obtained from CYMIT Química. Pyrrole (SAFC, ≥98% FCC) was distilled immediately before use. Ultrapure water employed in the preparation of the solutions was obtained from a Milli-Q system from Millipore. Carbon nanotubes were synthesized by the arc-discharge method using graphite electrodes and a Ni/Y 4/1 % metal catalyst mixture.

As-grown single-walled carbon nanotubes (agSWCNTs) were dispersed ultrasonically in aqueous 1% SDBS (initial nanotube concentration 4 mg/ml) and centrifuged at 13,000 rpm for 30 min (Hermle Z383) in order to increase their purity and decrease their metal content. The supernatant was decanted and the final concentration of nanotubes was estimated by UV–vis spectroscopy using absorbance at 600 nm (Shimazdu UV2401PC). For the construction of the calibration line, dilutions from the unpurified dispersions were used with a well-known concentration. The relative purity of the nanotubes in suspension was determined from near infrared (NIR) spectra (Bruker Vertex70 spectrometer). The NIR purity index was

calculated by comparing the baseline-corrected peak area corresponding to the interband S22 transition for the semiconducting nanotubes with the total area under the peak, as described in [39]. The final nanotube concentration resulted to be 1.5 mg/ml and the NIR purity index was 0.080.

Electrodeposition of the composite material was carried out in galvanostatic conditions using a current value of 3 mA cm-2 during 120 s, and the obtained transient is shown in figure 1. The polymerization solution was a 0.9% NaCl, 10-2 M total phosphate concentration, pH=7 phosphate buffer solution containing 3.5 10-3 M Sodium dodecylbenzene sulfonate (SDBS) and 0.15 mg/ml agSWCNTs. An Ag/AgCl (3 M NaCl) electrode was used as a reference electrode, and a graphite bar was used as a counter electrode. The quality of the film was checked using electrochemical impedance spectroscopy (EIS) in 0.9% NaCl, 10-2 M total phosphate concentration, pH=7 phosphate buffer solution, in a two-electrode configuration at a potential of 0V versus a graphite counter electrode and a decrease in the impedance modulus and phase were observed until a constant response.

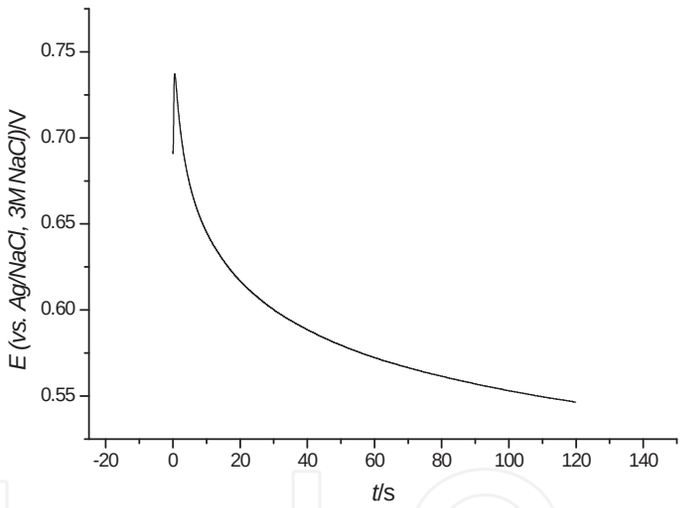

Figure 4. Galvanostatic transient obtained during the Ppy/SWCNT electrode deposition at a current of 3 mA cm^{-2}

2.3. Electrochemical impedance spectroscopy characterization

EIS was conducted by using a commercial impedance analysis system (SI 1260, Solartron Analytical) operated by Zplot software. Two-electrode impedance measurements were conducted to characterize the electrode-electrolyte interface impedance versus to a platinum reference electrode (Radiometer Analytical). The electrical properties of the electrode-electrolyte interface were evaluated by comparing the impedance and phase shifts to the frequency in physiological saline solution (0.9 wt.% NaCl, with a nominal resistivity of 71.3 Ωcm) in the 10 Hz to 1 MHz frequency range.

2.4. In vitro extracellular recordings

Coronal slices (0.4 mm thick) from occipital cortex and containing primary and secondary visual cortical areas [17, 18, and 19] were obtained from adult ferrets, as described in [40]. The MEA was inserted in the probe interface MEA1060, where the signal was pre-amplified. Further amplification (1000x) was obtained with amplifiers from Multichannel Systems. The artificial cerebrospinal fluid (ACSF) in which the slices were bathed contained (in mM): NaCl, 126; KCl, 3.5; MgSO4, 1; NaH2PO4, 1.25; CaCl2, 1.2; NaHCO3, 26; dextrose, 10, and was aerated with 95% O2, 5% CO2 to a final pH of 7.4. To induce spontaneous activity, a gabaergic blocker (5 μM) bicuculline methiodide (Sigma) was added at some point of the recording. The recording chamber where the slice was placed simulated an interface-style recording chamber, being closed on top and the air being humidified and enriched with oxygen. Bath temperature was maintained at 34.5 – 36 ºC.

3. Results and discussion

3.1. Electrochemical impedance spectroscopy electrode characterization

The neuronal activity is recorded as an extracellular potential or, as it is commonly called, an action potential. An action potential can be described as a short-lasting event in which the electrical membrane potential of a cell rapidly rises and falls. Specifically, in neurons, the action potentials play a central role in the cell-to-cell communication.

In an extracellular recording, the electrical activity detection is generated by the neurons adjacent to the electrode. Thus, the electrode area can be related with the number of neurons which activity can be detected. In general, recordings can be produced by the firing of a single neuron (single-unit activity) or can be generated by several neurons (multi-unit activity). In our case, the use of electrodes at the micro scale, gives the opportunity to detect signals of only one neuron. In living animals the single-unit recordings have provided insights into how does the brain processes information, while the multi-unit activity has usually been used to record changes during normal activity.

The use of MEAs, where the microelectrodes are closely spaced, provides the opportunity to register the activity of one neuron by several electrodes simultaneously. These recordings can be used to identify the number of neurons around each electrode as well as to locate the neurons in the space. This process is called spike sorting and is suitable in areas with well-defined spike characteristics where the type of cells is identified.

The main objective with the neuronal recording is to detect signals with a functional signal-to-noise ratio value of approximately 5:1 or greater in order to differentiate the neural activity from the background noise [41]. Therefore, the noise level represents a limit in the signals that can be detected. In general, two noise sources can be defined; the first one, known as neural noise, can be associated to the large amount of similar background action potentials produced by all the neurons surrounding the electrode. The second one, known as thermal noise, can be associated to the electrode impedance and is defined by equation 1:

http://dx.doi.org/10.5772/52174

$$V_{noise} = \sqrt{4 \cdot K_B \cdot T \cdot R \cdot \Delta f} \quad (1)$$

where K_B is the Boltzman Constant, T is the temperature, R is the real part of the impedance of the electrode and Δf the registered frequency range. It is important to note that only the real part of the impedance contributes to thermal noise. Consequently, for higher electrode impedances, lower signal-to-noise ratio will be obtained.

As it has been mentioned before, the use micro-electrodes with small area enables the possibility of recording activity from only one cell. However, this will increase the electrode impedance and so the associated thermal noise. Thus, it is necessary to use post-processing techniques in order to decrease the electrode impedance. As described in the previous section, the most accepted strategy is increasing the surface area of the electrode without modifying the effective area of the electrode. This can be achieved by increasing the roughness of the electrode surface. By this strategy the thermal noise will be reduced, and the electrode impedance characterization will become a powerful tool to analyze the neural behaviour and to enable the comparison between electrodes.

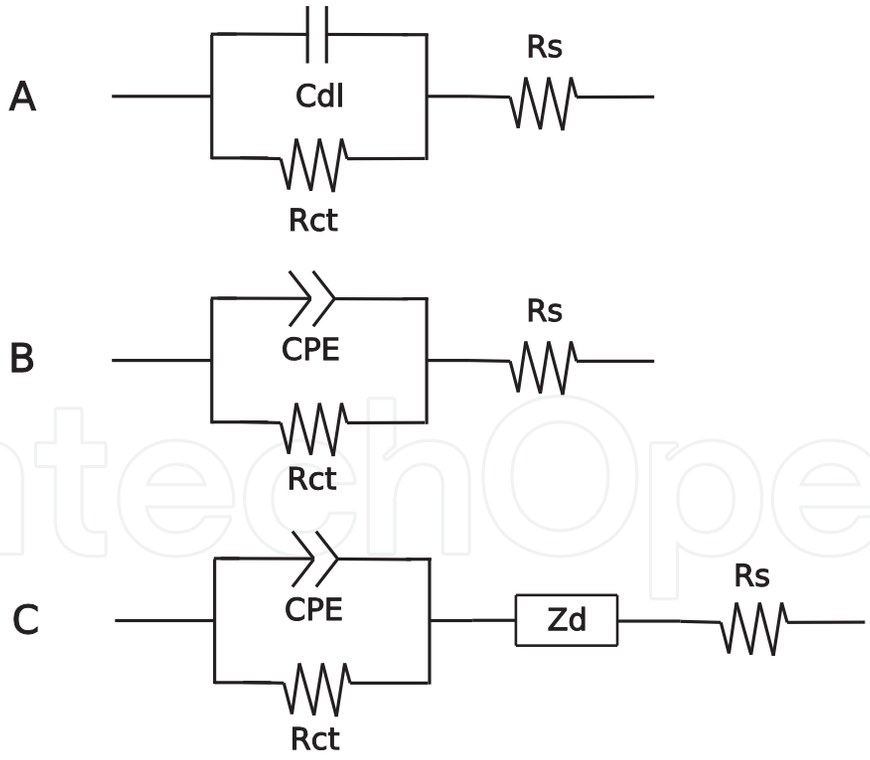

Figure 5. Equivalent circuits used to fitting the EIS characterization data. A) Simplest model where the double layer is modelled with a pure capacitance. B) Model used to fit the measurements of Pt, BkPt and dcSWNT electrodes, where the double layer behaviour is modelled by a CPE component instead of the pure capacitance. C) Model used to fit the measurements of the grMWNT and ppy/SWNT electrodes where have been added a Zd impedance to model the diffusion impedance produced by the porous thin film modifications.

In order to better understand the electrode characterization that will be hold in this section, a brief introduction of the Electrochemical Impedance Spectroscopy (EIS) technique as a tool to characterize electrode-electrolyte interface will be given. This method is based on the application of an AC potential (E(t) = Eo cos(ω + t)) of small amplitude (typically E_0 = 10 mV) that generates an AC current, I (t) = I0 cos(ωt −φ). From the relation of both signals the impedance (Z) is defined (Z= E(t)/I(t)). The obtained impedance data results in a complex number (Z= Z_{real} + j Z_{imag}), which is needed to express the signal attenuation (impedance modulus) and the delay between signals (impedance argument) in a same number. The measurements are carried out at different AC frequencies, and thus the name of impedance spectroscopy. Moreover, from the two ways to plot the impedance data, the Bode Plot, used to represent the polar notation of the complex number, has been chosen to show the data in this work. There, the impedance modulus $|Z|$ and the phase shift angle φ are represented as a function of the frequency ω usually in a logarithmic scale (i.e. Fig 6). In this plot, the resistive processes show a phase angle close to 0 and a flat modulus behaviour, whereas the ones that are dependent on the frequency are more related to capacitive or diffusive processes (phase angles between -90º and -45º). As a result, the impedance spectra can give us a broad overview of the different processes taking place at the electrochemical interface (capacitive, resistive, diffusion effects) showing which one is dominating at a specific range of frequencies.

Figure 5 shows several equivalent circuits that can be used to understand the electrode-electrolyte processes. The equivalent circuit models can be divided in two parts, one related to the access resistance and the other to charge transfer at the electrode double layer. The components used to describe each phenomenon depend on the electrode materials properties. The first approach (model A, Fig. 5A) describes the double layer behaviour as a pure capacitance *Cdl* in parallel combination with the charge transfer resistance *Rct*. In our case this last value is infinitely large (> 10^{10} ohm) and therefore it can be omitted. The access resistance is modelled by the solution resistance *Rs* that mainly depends on the geometric area of the electrode and the conductivity of the solution. Based on this model the impedance modulus at 1 kHz is generally used by neurophysiologists as an indicator of the electrode quality.

However this approximation can only describe the electrode behaviour in all the frequency range when the electrode-electrolyte interface behaves as a pure capacitance. To achieve a better representation of the dissipative double layer behaviour it is necessary to substitute the pure capacitance by a faradaic pseudocapacitance known as the constant phase element CPE (model B, Fig. 5B). The impedance of this CPE is defined in the following equation:

$$Z_{CPE}(\omega) = \frac{1}{q(j\omega)^n} \tag{2}$$

http://dx.doi.org/10.5772/52174

where j = √-1 and ω is the angular frequency in rad s^{-1}. Moreover, the CPE is defined by two parameters; *q* and *n*. *q* indicates the value of the capacitance of the CPE when *n* approaches to 1, while *n* can be correlated with several factors like the surface roughness and a non-uniform current distribution as the more important ones. For *n*=1, CPE describes an ideal capacitor and for *n*=0, CPE describes an ideal resistor.

The third model (model C, Fig. 5c) is related to the electrode modification with conducting polymer films. This approximation introduces diffusion processes in the electrode surface that can be modelled by the inclusion of Z_d impedance in the described equivalent circuit. Diffusion processes in polymer coatings are usually modelled by transmission lines. These models were first proposed by de Levie [42] for porous electrodes and Bisquert et al. [23,24], who applied this theory for the thin film coatings. Thus, the diffusion impedance Zd is generally described by

$$Z_d(\omega) = \left(\frac{R}{\sqrt{\Lambda}}\right)\coth(\sqrt{\Lambda})$$
$$\Lambda = 1/R_1 + Q_1(j\omega)^{\varphi} \tag{3}$$

where *R* gives the resistance of the ionic pores of the film; while the R_1, Q_1 and φ, represents the charge transfer at the electrolyte polymer interface at the pores wall.

The experimental results for the different proposed electrodes; bare platinum (Pt), electrodeposited black platinum (BkPt), drop casted SWNTs (dcSWNT), grown MWNTs (grMWNT) and electrodeposited ppy/SWNT composite (ppy/SWNT), have been fitted (Figure 6) to the above described equivalent circuits. The model B was used in the case of Pt, BkPt and dcSWNTs, which behaviour do not present any diffusion process at the electrode-electrolyte interface (Fig. 6 left). On the other hand, the model C was used for the electrodes modified with grMWNT or ppy/SWNT as they present a porous thin film coating than can be associated to an impedance diffusion behaviour (Fig. 6 right). It can be observed the goodness of the fitting in both cases. In Table 1 the obtained values for each parameter of the model is shown.

As expected, the increase of the electrode surface roughness due to all the proposed post-processing techniques lead to a decrease in the initial impedance modulus approximately a 10-fold. This is as a direct consequence of the enlargement of the effective surface area which can be reflected on the equivalent capacitance value of the CPE, increasing from 1 E-9 of the Pt electrode to 2.1 E-7 for the ppy/SWNT (detailed values of *q* in Table 1). It is important to note that the *n* values of the CPE found are significantly lower than 1, demonstrating that using a CPE component is better than using a pure capacitive one. Furthermore, as can be observed in Table 1, the calculated thermal noise according to eq. (1) is reduced from 3.1 μV for the bare platinum to 1.2 -1.5 μV for the modified electrodes. This increase of the signal-to-noise ratio is one of the main reasons for the neural recording improvement.

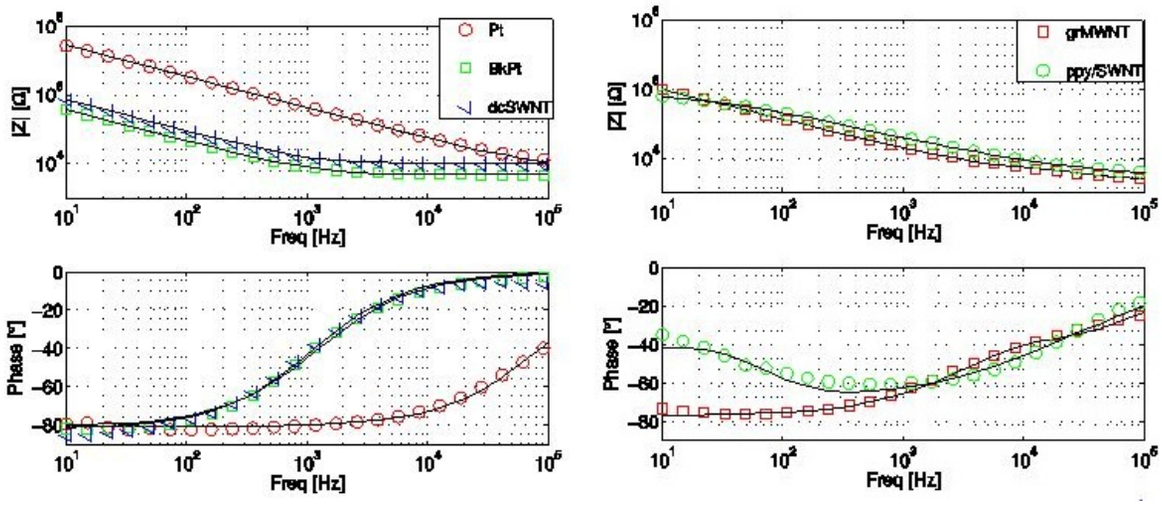

Figure 6. Bode plot (left) of electrochemical impedance of bare platinum electrodes (Pt), electrodeposited black platinum (BkPt) and drop casted SWNTs (dcSWNT). Bode plot (right) of electrochemical impedance of grown MWNTs (grMWNT) and electrodeposited ppy with SWNTs (ppy/SWNT). The fitting results are shown by the solid line, electrodes represented in the left are fitted to the proposed model B and electrodes represented in the right are fitted to the proposed model C.

From Table 1 it can be noticed, that the *Rs* value of the modified electrodes are lower than the value corresponding to the bare platinum electrode. Albeit the *Rs* of BkPt and dcSWNT (7.0 kΩ) are similar to the bare Pt electrode (7.6 kΩ), the values of the grSWNT (2.1 kΩ) and the ppy/SWNT (4.2 kΩ) present a significant reduction. Taking into account, as it has been mentioned before, that *Rs* mainly depends on the electrode area and the conductivity of the solution, which can be assumed to be the same for all cases, the observed variations on this parameter could be considered as an expansion of the real surface area. This assumption is based on a phenomenon that has been previously reported by Abidian et al. [34] and Lu et al. [43].

Parameter	Unit	Pt	BkPt	dcSWNT	grMWNT	ppy/SWNT
|Z| (at 1 kHz)	Ω	3,9E+5 ± 1,7E+5	6,1E+4 ± 5,0E+4	1,4E+4 ± 3,0E+3	3,0E+4 ± 7,1E+3	3,3E+4 ± 1,8E+4
q	μFs^{n-1}	1,0E-9 ± 5,4E-10	3,3E-8 ± 4,8E-8	3,3E-8 ± 1,0E-8	1,9E-8 ± 5,4E-9	2,1E-7 ± 4,1E-8
n	$0 \leq n \geq 1$	0,900 ± 0,001	0,899 ± 0,002	0,898 ± 0,017	0,856 ± 0,003	0,627 ± 0,054
Rs	Ω	7,6E+3 ± 1,6E+3	7,0E+3 ± 1,9E+3	7,0E+3 ± 1,5E+2	2,1E+3 ± 3,0E+2	4,2E+3 ± 1,1E+3
R	Ω	—	—	—	1,9E+2 ± 1,9E+2	8,0E+2 ± 7,0E+2
R_1	Ω	—	—	—	5,3E+1 ± 3,9E+1	4,7E+2 ± 3,0E+2
Q_1	$\mu Fs^{\varphi-1}$	—	—	—	8,3E-6 ± 7,5E-6	3,1E-5 ± 4,7E-5
φ	$0 \leq \varphi \geq 1$	—	—	—	0,722 ± 0,033	0,952 ± 0,026
Thermal noise	V	3,1E-6 ± 8,4E-7	1,4E-6 ± 3,7E-7	1,2E-6 ± 5,5E-8	1,3E-6 ± 1,6E-7	1,5E-6 ± 3,5E-7
Fittinig model	—	B	B	B	C	C

Table 1. Experimental results and fitting parameters for impedance measurements shown in Figure 6.

http://dx.doi.org/10.5772/52174

For the electrodes that present diffusion processes, grMWNT and ppy/SWNT, the contribution to the total impedance measurement of the CPE parameter and the *Zd* has been separated. This is shown in Figure 7 where it can be observed that the contribution at the low frequency range of *Zd* is significantly higher for the ppy/SWNT coating than for the grMWNT case. However, at high frequencies the *Zd* contribution of ppy/SWNT is lower. Then, it can be stated that for the case of grMWNT the low frequency range is dominated by the CPE behaviour while the high frequency range is dominated by the *Zd* behaviour. On the contrary, in the case of ppy/SWNT the low frequency range is dominated by the *Zd* behaviour and at high frequency range is dominated by the CPE behaviour. This different behaviour can probably be attributed to the small pores that the grMWNT based electrode presents. Fig. 8B shows a SEM image of the vertically aligned MWNTs from where its porous morphology can be related to two causes: the separation between nanotubes (estimated as 10-15 nm after SEM imaging) and the own carbon nanotube inner diameter (typically observed to be 2-3 nm after TEM imaging). The presence of these small diameter pores suggests that ions may not pass through them at low frequency ranges; hence, the active area is only related to the superficial area assuming a CPE behaviour in these frequencies. On the other hand, and as it can be observed in Fig 8D, the ppy/SWNT coating presents less compact porous morphologies with bigger pores. This is also reflected in the *n* value of the CPE (0.627) suggesting a high superficial roughness.

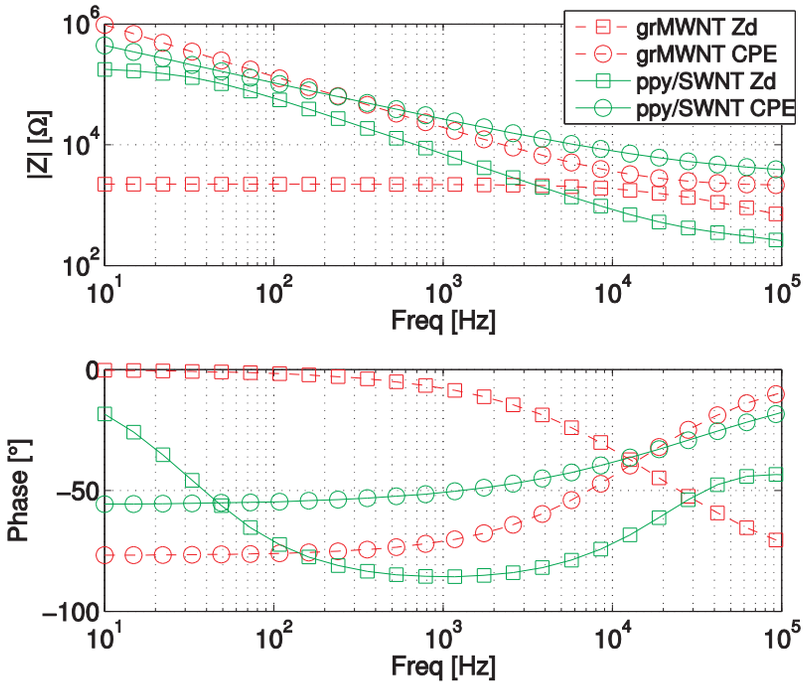

Figure 7. Detailed Bode plot where the total measured impedance of the grMWNT and the ppy/SWNT has been separated into the contribution of the CPE parameter (circles) and the Zd (squares).

The SEM images shown in Figure 8 are useful to relate the morphologies of the above proposed materials for the electrode modification with the parameters of the different impe-

dance models that have been already discussed. The black platinum, BkPt, (Fig. 8A) acquires a fractal structure when it is electrodeposited. This structure contains numerous sub-micrometer even nanometer particles that contribute to increase the final effective surface area, which, sometimes, acquires a cauliflower-like structure. The grown multi-walled carbon nanotubes, grMWNT, (Fig. 8B) consist in a high density of vertically-aligned CNTs that remain stable thanks to Van der Waals forces. These CNTs, depending on the fabrication process, usually have an inner diameter of about 2-3 nm, and an inter-tube space of 10-15 nm. This structure confers to this type of electrode a high porosity all along the length of the CNTs. Albeit the topographical surface of the grMWNTs seems less rough than the surface obtained with the black platinum electrodeposition, the individual tips of the nanotubes at a nanometer scale, highly contribute to the surface roughness. Consequently, the effective surface area of the grMWNT can be considered as a sum of the electrolyte-CNT walls interface and the electrolyte-CNTs tips interfaces.

The drop-casted SWNTs (Fig. 8C) present the typical spaghetti-like structure where the individual nanotubes are entangled producing a compact material. It can be observed that this type of modification does not produce a porous material; only the small diameter (1-2 nm) of the individual SWNTs contribute to an increase of the effective surface area, in a similar way as the black platinum coating. In contrast, the ppy/SWNTs (Fig. 8D) exhibit a very different morphology. A three-dimensional porous microstructure formed by the individual nanotubes covered by the polypyrrole film can be discerned. Because of the diameter of the individual SWNTs (in the range of 1-2 nm), and assuming that they can be grouped in ropes, the thickness of the structures observed in the microscope is basically due to a thick polymer layer.

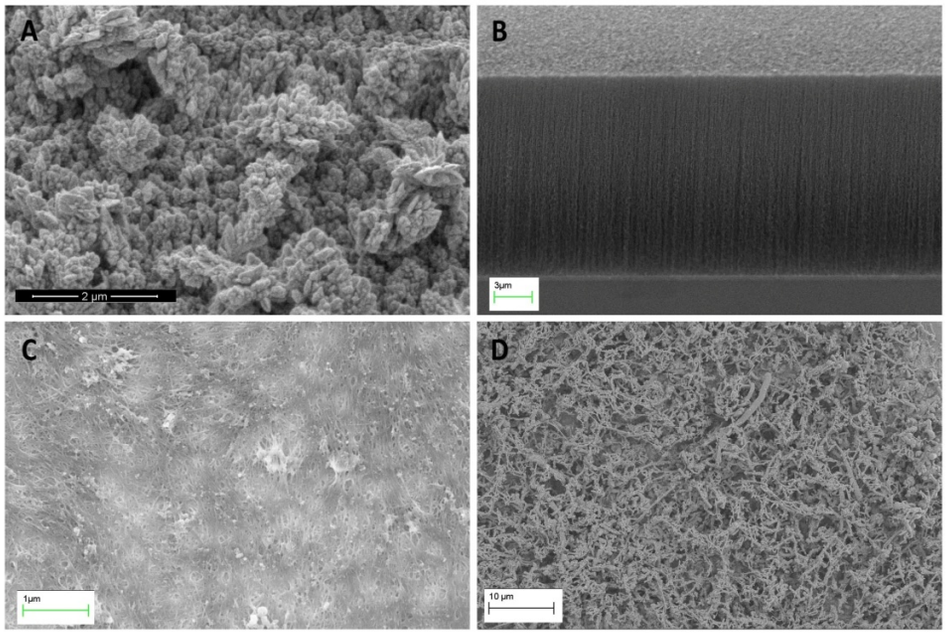

Figure 8. SEM images of the different materials used for the electrode modification surface, A) electrodeposited black platinum; B) grown MWNTs; C) drop casted SWNTs; D) electrodeposited ppy/SWNTs composite.

As a general conclusion of the electrochemical impedance spectroscopy characterization it can be stated that the different proposed post-processing strategies lead to an impedance improvement of approximately 10-fold reduction with respect to the initial bare electrode impedance values. This is especially beneficial for the neural recording electrodes as it supposes a reduction of the thermal noise value and, therefore, a better signal-to-noise ratio. Despite the similar electrochemical characteristics of the described electrodes, the main weakness of the electrodeposited black platinum is its lack of adhesion to the electrode, which compromises its mechanical stability [1]. As expected, this issue affects negatively to the recording electrodes and constitutes a limitation for the electrode reusability as the detachment of the black platinum due to the friction between the electrode and the tissue produces a progressive increase of the electrode impedance.

The motivation for using CNTs is based on the need for finding an alternative electrode improvement method that fulfils the two requirements; low-impedance electrode interface and good mechanical stability required for successful long term recordings. Here, it has been demonstrated that the CNTs modifications present the same good electrical properties as the black platinum along with good mechanical stability of this material that has been previously reported [11, 44, 45].

3.2. In vitro recordings with standard and flexible MEAs

The use of standard rigid MEAs poses problems for the recordings from cortical slices. It is especially problematic if the purpose is not the recording of stimulus-evoked responses but of spontaneously generated activity. The generation of specific patterns of activity in cortical slices, such as slow [40] and fast [46] rhythms requires an optimal state of the cortical slices. The generation of these patterns of activity also requires brain tissue from adult rather than juvenile rats [47], which is always more vulnerable and sensitive to factors such as low oxygenation. The main problem that we have encountered with the use of standard MEAs is the combination of ACSF (artificial cerebrospinal fluid) flow under the slice with a good and continued contact of the electrodes with the tissue. This is an easy problem to understand: the brain tissue in the form of a cortical slice is 400 micrometers thick and has to be continuously bathed and oxygenated. Dryness is a killer to the tissue. Given that the standard MEAs have flat electrodes, the key of a good electrical recording resides on a close contact between the electrode and the tissue. However, to keep the slices alive, liquid has to be flowing between the electrodes and the tissue, what not only increases the distance between the electrodes and the slice, but also compromises the mechanical stability that guarantees that the recording is always obtained from the same point.

To deal with these problems we used different strategies: one was to cut the slices thinner down to 300 micrometers, with the objective that the fluid over the slice would be enough to keep the area under bathed and oxygenated. However, even with thinner tissue this problem was not solved. Another strategy that we used in order to bath the slice while maintaining mechanical stability was to put a thin stripe of filter paper on top of the slice and thus keeping the slice in place while the fluid was circulating through the filter paper. This was also helpful to create a kind of interface chamber, which has advantages to maintain slices

active and well oxygenated [47,48]. Still, under these conditions there was a loss of activity probably due to the deterioration of the tissue in area in contact with the electrodes.

An strategy used by others (Multichannel systems) to circumvent these issues has been to create a perforated base that is used with negative pressure and thus suction of the slice from below, thus achieving mechanical stability and probably maintaining a warm, humid and oxygenated environment at the bottom of the brain slice. We do not have firsthand experience with this system and we cannot say if it fulfils its purpose.

In spite of all these problems, we were able sometimes to obtain good recordings with the MEAs, and in particular with those modified with grMWNTs (Figure 9b). In Figure 9B we were able to record epileptiform activity induced by the blockade of $GABA_A$ receptors. We think that the grMWNTs makes possible a better contact of the electrode with the tissue thanks to the height of the carbon nanotubes. Still, the recordings did not last long and were not comparable to what is achieved in the same slices with conventional needle-like tungsten electrodes, where recordings can last for several hours.

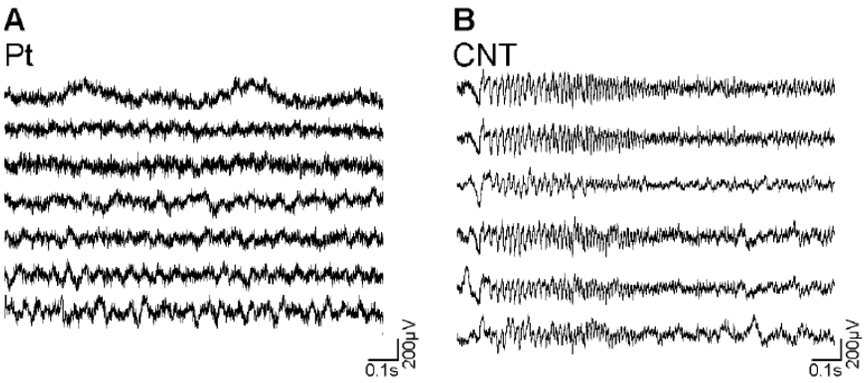

Figure 9. Recordings of spontaneous activity in the slice with Pt electrodes (a) and with grMWNT (b). An oscillation resulting from the gabaergic blockage has been recorded with the CNT-MEA. Recordings have been high passed filtered (1000 Hz) equally in (a) and (b).The same gain (x1000) and filters were used in (a) and (b), while also in both cases 50 µM bicuculline ($GABA_A$ receptor blocker) was present in the bath. Notice an epileptiform discharge in (b). Taken with permission from (20).

Given all the problems encountered with the standard rigid MEAs, we decided to try flexible MEAs that could be positioned on top of the slices in their standard interface chamber. These offers a number of advantages from the point of view of maintaining the tissue alive [47]: there is a good ACSF flow, critical for maintaining the correct ionic and glucose levels as well as temperature and oxygenation, both critical for the normal generation of cortical emergent activity [48]. Furthermore, the filter paper used on the base of interface chambers confers the slice a complete mechanical stability, making unnecessary any other kind of fixation mechanisms. A healthy brain tissue is the basis for a good electrophysiological recording. Once this is achieved, we can place the flexible MEA on top of the slice. We achieve this by means of a micromanipulator. In our experience, the flexible MEA can be held in place. Even when initially there may be problems of stability and the MEA may slip on the surface,

http://dx.doi.org/10.5772/52174

once it settles we can obtain stable recordings for a few hours (Figures 10, 11). In Figure 10 we illustrate 5 out of 16 channels recording with our flexible MEAs. The LFP (local field potential) signal shows the ocurrence of three cycles of a spontaneous slow oscillation [40], while at the bottom a high pass filtered channel illustrates the multiunit activity corresponding to the spikes of local neurons. Because this is a flexible MEA and it is at an angle to lie on the tissue, there is a certain pressure made by the MEA on the slice. Even when we cannot measure what that pressure is, we know that it is enough to guarantee a good contact with the electrodes and to maintain the MEA in place. However, the pressure is not too much as to induce any damage on the brain tissue, indeed allowing several hours of successful recordings.

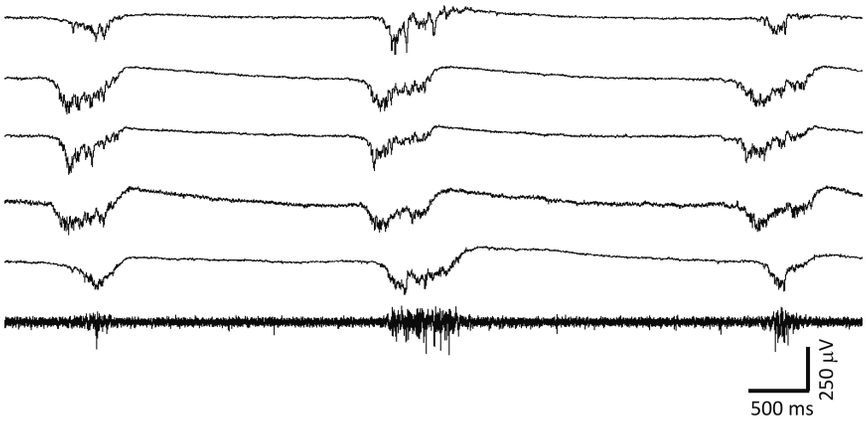

Figure 10. Recordings obtained with a flexible MEA with Pt electrodes. In five channels the LFP (local field potential) are illustrated (unfiltered). In the bottom channel the signal has been high pass filtered (500 Hz) and shows the multiunit activity. The activity of the slice corresponds to a slow oscillation that has 3 cycles in the figures. This activity is spontaneous and is a sign of the good physiological state of the cortical slice. An indication of the good quality of the physiology and the recording is the generation of high frequencies during each cycle, which are visible during the periods of activity (LFP going down).

Once we knew that the flexible MEAs had advantages over the rigid MEAs, we explored the effect of depositing CNTs on the recording points. This was the reason for trying the ppy/SWNTs electrodeposition option, as a way to fabricate electrodes with low-impedance values. As we have said above, this induces a decreased impedance of the electrodes without increasing their size. Decreasing the impedance without increasing the size of the recording point, but increasing the surface is a used strategy to obtain recordings from a small area without high electrical noise [49]. Even when we have not carried out specific measurements of signal to noise, flexible MEAs with carbon nanotubes obtained not only with low noise, but with a good detection of high frequencies (see Figure 11). During the cycles of activity of the slow oscillations, there is local synchronization in high frequencies (30-80 Hz; [46]). In Figure 11 we illustrate that the electrode with NT allowed a good view of these high frequency oscillations during the three cycles of activity displayed. Furthermore, we were able to record with this surface electrode single neurons in the multiunit channel (Figure 11, bottom trace), similarly to the recordings obtained with plated electrodes [49]. Obtaining single units with surface electrodes is unusual. Normally to obtain single units (recording axons for isolated neurons) other

techniques need to be used, such as sharp glass-pulled electrodes or plated tungsten electrodes [49] that are placed inside the brain tissue rather than in the surface.

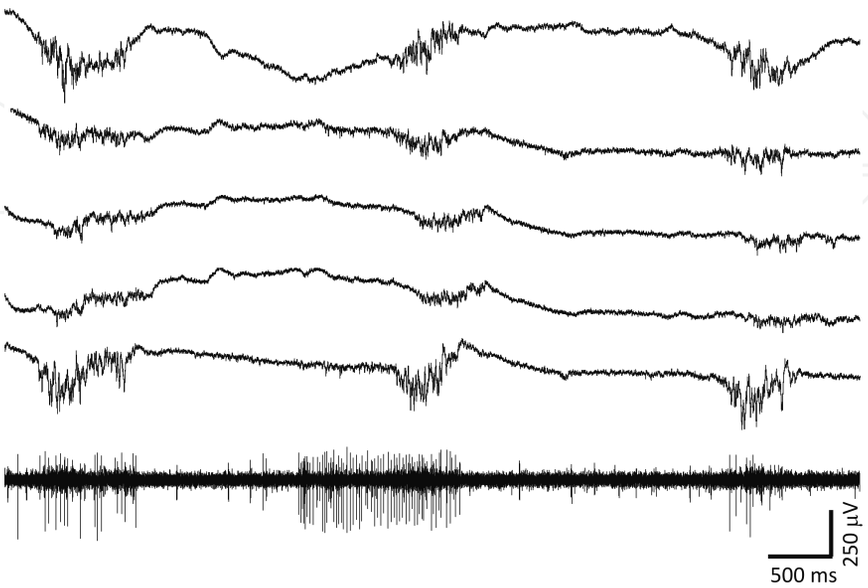

Figure 11. Recordings obtained with a flexible MEA with grMWNTs. In five channels the LFP (local field potential) are illustrated (unfiltered). In the bottom channel the signal has been high pass filtered (500 Hz) and shows multiunit activity. The activity of the slice corresponds to a slow oscillation that has 3 cycles in the figures. This activity is spontaneous and is a sign of the good physiological state of the cortical slice. An indication of the good quality of the physiology and the recording is the generation of high frequencies during each cycle, which are visible during the periods of activity (LFP going down).

We therefore find that for recording spontaneous rhythmic activity from brain slices flexible MEAs yield in our hands better results than rigid MEAs. Furthermore, we find that using CNTs as electrode interface may be a promising technique to obtain high quality electrophysiological recordings from the surface of brain slices.

4. Conclusions

It is a fact that several probe technologies have supposed a revolution on our understanding of the brain behaviour by revealing us how the network neurons work. Because the trend in the neurology field is having a large number of electrodes (MEA devices) arranged closely, that could provide local registering and stimulation, the investigation in the MEA fabrication devices have become a challenge to work in.

Related to the use of microelectrodes for neuronal recordings, one of the main objectives is to achieve low-impedance interfaces. Furthermore, the most important milestone that must be overcome, is maintaining these low-impedance properties. Here we have presented several post-processing strategies in order to decrease the microelectrode impedance. One of the most common ways to achieve it is the black platinum electrodeposition (61 kΩ at 1 kHz). However,

http://dx.doi.org/10.5772/52174

the electrochemical response in a long term experiment is not stable for this material due to the platinum detachment. As an alternative there are techniques such as the use of hydrogel coatings that can be used to solve this problem. However we have proposed several carbon nanotube post-processes (drop casted CNTs and CNTs growth) that achieve the low impedance requirements and remain stable during acute recordings (14 kΩ and 30 kΩ at 1 kHz). This is especially beneficial to the neural recording electrodes because it supposes a reduction of the thermal noise value and as a consequence a better signal-to-noise ratio.

In this chapter we have tried to highlight that besides the impedance requirements that the microelectrodes must fulfill and that these values must be maintained for successful chronically experiments, the standard rigid MEAs deal with several other problems. In order to obtain good recordings the electrodes must be in closer contact with the brain slices and the tissue must be maintained alive. These two items have turned against the silicon standard photolithographic technologies, and has favoured the investigation on the polymer micro technologies. So, here it has been proposed the MEA fabrication in SU-8 polymer, which has the properties of being transparent, flexible and low cost. The fabrication of 25 μm thick probes has enabled the possibility to obtain acute recordings for a long period of time. However, in the case of SU-8 probes, impedance improvement strategies have been adapted to the SU-8 material properties. So, it has also been compared the common electrodeposition technique of black platinum to the electrodeposition of a composite of SWNTs and the polymer polypyrrole. The composite overcomes the usual mechanical stability problems reported before for the black platinum. The impedance properties achieved with this composite are very interesting. It presents a low impedance value at 1 kHz (33 kΩ), and a significant diffusion phenomenon consequence of its porous morphologies. This is an important characteristic in the case of microelectrodes used in stimulation, because it is responsible of increasing the safe charge injection limit (Qinj) that establishes differences between stimulating electrodes.

Acknowledgements

RV work has been funded by the project SAF2009-14724-C02-02 co-financed by the Spanish Ministry of Science and Innovation and the European Regional Development Fund. Also the GICSERV Program (6th call), Funded by MICINN has co-financed this work.

MVSV work was supported by Ministerio de Economía y Competitividad (Spain) BFU2011-27094.

MTM wish to thank Spanish Ministry of Science and Innovation (MICINN) and the European Regional Development Fund (ERDF) for financial support under project MICINN TEC2010-15736, and Mercedes Vico-Gallardo for her dedicated and helpful work. J.H.F. acknowledges the Spanish Superior Council for Scientific Research (CSIC) for his JAE-Doc contract

Author details

Gemma Gabriel[1,2*], Xavi Illa[1,2], Anton Guimera[1,2], Beatriz Rebollo[4], Javier Hernández-Ferrer[3], Iñigo Martin-Fernandez[1], Mª Teresa Martínez[3], Philippe Godignon[1,2], Maria V. Sanchez-Vives[4,5] and Rosa Villa[1,2]

1 Instituto de Microelectrónica de Barcelona (IMB-CNM), CSIC, Campus UAB, Barcelona, Spain

2 CIBER-BBN, Networking Center on Bioengineering, Biomaterials and Nanomedicine, Spain

3 Instituto de Carboquímica (CSIC), C/Miguel Luesma Castán 4, Zaragoza, Spain

4 IDIBAPS (Institute of Biomedical Research August Pi y Sunyer), Barcelona, Spain

5 ICREA (Institut Catala de Recerca i Estudis Avançats), Barcelona, Spain

References

[1] Fejtl, M., Stett, A., Nisch, W., Boven-H, K., & Möller, A. (2006). Advances in Network Electrophysiology. *Springer US*, cited 2012 Mar 22, 24-37.

[2] Pine, J. (2006). Advances in Network Electrophysiology. *Springer US*, cited 2012 Mar 22, 3-23.

[3] Whitson, J., Kubota, D., Shimono, K., Jia, Y., & Taketani, M. (2006). Advances in Network Electrophysiology. *Springer US*, cited 2012 Mar 22, 38-68.

[4] Liu, X., Yue, Z., Higgins, MJ, & Wallace, G. G. (2011). Conducting polymers with immobilised fibrillar collagen for enhanced neural interfacing. *Biomaterials*, Oct, 32(30), 7309-17.

[5] Lee, J. Y., Bashur, C. A., Goldstein, A. S., & Schmidt, C. E. (2009). Polypyrrole-coated electrospun PLGA nanofibers for neural tissue applications. *Biomaterials.*, Sep, 30(26), 4325-35.

[6] Ghasemi-Mobarakeh, L., Prabhakaran, M. P., Morshed, M., Nasr-Esfahani, M. H., & Ramakrishna, S. (2009). Electrical Stimulation of Nerve Cells Using Conductive Nanofibrous Scaffolds for Nerve Tissue Engineering. *Tissue Engineering Part A.*, Nov, 15(11), 3605-19.

[7] Gerwig, R., Stett, A., & Stelzle, M. (2012). PEDOT-CNT composite microelectrodes for recording and electrostimulation applications: fabrication, morphology, and electrical properties. *Front. Neuroeng*, 5, 8.

[8] Cellot, G., Cilia, E., Cipollone, S., Rancic, V., Sucapane, A., Giordani, S., et al. (2009). Carbon nanotubes might improve neuronal performance by favouring electrical shortcuts. *Nat Nano.*, Feb, 4(2), 126-33.

[9] Shoval, A., Adams, C., David-Pur, M., Shein, M., Hanein, Y., & Sernagor, E. Carbon Nanotube Electrodes for Effective Interfacing with Retinal Tissue. *Front Neuroengineering*, 2.

[10] Keefer, E. W., Botterman, B. R., Romero, M. I., Rossi, A. F., & Gross, G. W. (2008). Carbon nanotube coating improves neuronal recordings. *Nat Nano*, Jul, 3(7), 434-9.

[11] Voge, C. M., & Stegemann, J. P. Carbon nanotubes in neural interfacing applications. *Journal of Neural Engineering.*, 8(1), 011001.

[12] Jorio, A., Dresselhaus, G., & Dresselhaus, MS. (2008). Carbon nanotubes: advanced topics in the synthesis, structure, properties and applications. *Springer*.

[13] Reich, S., Thomsen, C., & Maultzsch, J. (2008). Carbon Nanotubes: Basic Concepts and Physical Properties. *John Wiley & Sons*.

[14] Malarkey, E. B., & Parpura, V. (2007). Applications of carbon nanotubes in neurobiology. *Neurodegener Dis*, 4(4), 292-9.

[15] Malarkey, E. B., & Parpura, V. (2010). Brain Edema XIV. *Springer Vienna*, cited 2012 Mar 22, 337-341.

[16] Gabriel, G., Gómez, R., Bongard, M., Benito, N., Fernández, E., & Villa, R. (2009). Easily made single-walled carbon nanotube surface microelectrodes for neuronal applications. *Biosensors and Bioelectronics.*, Mar 15, 24(7), 1942-8.

[17] Gabriel, G., Gomez-Martinez, R., & Villa, R. (2008). Single-walled carbon nanotubes deposited on surface electrodes to improve interface impedance. *Physiological Measurement*, S203-S212.

[18] Martin, I., Rius, G., Gabriel, G., Esplandiu, MJ, Mestres, N., Perez-Murano, F., et al. (2007). Local growth of carbon nanotubes by thermal chemical vapor deposition from iron based precursor nanoparticles. *Electron Devices, Spanish Conference on [Internet].*, cited 2010 Aug 25, 329-332.

[19] Martin-Fernandez, I., Gabriel, G., Rius, G., Villa, R., Perez-Murano, F., Lora-Tamayo, E., et al. (2009). Vertically aligned multi-walled carbon nanotube growth on platinum electrodes for bio-impedance applications. *Microelectronic Engineering*, 86(4-6), 806-808.

[20] Martin-Fernandez, I., Gabriel, G., Palomer, X., Reig, R., Sanchez-Vives, Villa. R., et al. Standardized fabrication of MWNTs-based MEA with biocompatible materials for emergent activity in the cortical network. *Biosensors & Bioelectronics.*, Submitted.

[21] Marrese, C. A. (1987). Preparation of strongly adherent platinum black coatings. *Analytical Chemistry. Enero*, 59(1), 217-8.

[22] Robinson, D. (1968). The electrical properties of metal microelectrodes. *Proceedings of the IEEE*, 56(6), 1065-1071.

[23] Rodger, D. C., Fong, A. J., Li, W., Ameri, H., Ahuja, A. K., Gutierrez, C., et al. (2008). Flexible parylene-based multielectrode array technology for high-density neural stimulation and recording. *Sensors and Actuators B: Chemical.*, Jun 16, 132(2), 449-60.

[24] Lacour, S., Benmerah, S., Tarte, E., Fitz, Gerald. J., Serra, J., Mc Mahon, S., et al. (2010). Flexible and stretchable micro-electrodes for in vitro and in vivo neural interfaces. *Medical and Biological Engineering and Computing*, 48(10), 945-54.

[25] Rousche, P. J., Pellinen, D. S., Pivin Jr, D. P., Williams, J. C., Vetter, R. J., & Kipke, D. R. (2001). Flexible polyimide-based intracortical electrode arrays with bioactive capability. *IEEE Transactions on Biomedical Engineering*, 48(3), 361-70.

[26] Metz, S., Bertsch, A., Bertrand, D., & Renaud, P. (2004). Flexible polyimide probes with microelectrodes and embedded microfluidic channels for simultaneous drug delivery and multi-channel monitoring of bioelectric activity. *Biosensors and Bioelectronics*, 19(10), 1309-18.

[27] Stieglitz, T., Beutel, H., Schuettler, M., & Meyer, J. (2000). Micromachined, Polyimide-Based Devices for Flexible Neural Interfaces. *Biomedical Microdevices*, 2, 283-94.

[28] Takeuchi, S., Ziegler, D., Yoshida, Y., Mabuchi, K., & Suzuki, T. (2005). Parylene flexible neural probes integrated with microfluidic channels. *Lab on a Chip Miniaturisation for Chemistry and Biology*, 5(5), 519-23.

[29] Tijero, M., Gabriel, G., Caro, J., Altuna, A., Hernández, R., Villa, R., et al. (2009). SU-8 microprobe with microelectrodes for monitoring electrical impedance in living tissues. *Biosensors and Bioelectronics*, 24(8), 2410-6.

[30] Altuna, A., Menendez la, Prida. L., Bellistri, E., Gabriel, G., Guimerá, A., Berganzo, J., et al. (2012). SU-8 based microprobes with integrated planar electrodes for enhanced neural depth recording. *Biosensors and Bioelectronics*, 37(1), 1-5.

[31] Green, R. A., Lovell, N. H., Wallace, G. G., & Poole-Warren, L. A. (2008). Conducting polymers for neural interfaces: challenges in developing an effective long-term implant. *Biomaterials.*, Sep, 29(24-25), 3393-9.

[32] Poole-Warren, L., Lovell, N., Baek, S., & Green, R. (2010). Development of bioactive conducting polymers for neural interfaces. *Expert Rev Med Devices.*, Jan, 7(1), 35-49.

[33] Hernández-Ferrer, J., Ansón-Casaos, A., & Martínez, M. T. (2012). Electrochemical synthesis and characterization of single-walled carbon nanotubes/polypyrrole films on transparent substrates. *Electrochimica Acta*, Mar 1, 64(0), 1-9.

[34] Abidian, M. R., & Martin, D. C. (2008). Experimental and theoretical characterization of implantable neural microelectrodes modified with conducting polymer nanotubes. *Biomaterials.*, Mar, 29(9), 1273-83.

[35] Chen-H, C., Chuang-C, S., Su-C, H., Hsu-L, W., Yew-R, T., Chang-C, Y., et al. (2011). A three-dimensional flexible microprobe array for neural recording assembled

through electrostatic actuation. *Lab on a Chip- Miniaturisation for Chemistry and Biology*, 11(9), 1647-55.

[36] Fernandez, L. J., Altuna, A., Tijero, M., Gabriel, G., Villa, R., Rodríguez, MJ, et al. (2009). Study of functional viability of SU-8-based microneedles for neural applications. *Journal of Micromechanics and Microengineering*, 19(2).

[37] Altuna, A., Gabriel, G., De La Prida, L. M., Tijero, M., Guimerá, A., Berganzo, J., et al. (2010). SU-8-based microneedles for in vitro neural applications. *Journal of Micromechanics and Microengineering*, 20(6).

[38] Ivorra, A., Gómez, R., Noguera, N., Villa, R., Sola, A., Palacios, L., et al. Minimally invasive silicon probe for electrical impedance measurements in small animals. *Biosens Bioelectron.*, 19(4), 391-9.

[39] Zhao, B., Itkis, M. E., Niyogi, S., Hu, H., Perea, D. E., & Haddon, R. C. (2004). Extinction Coefficients and Purity of Single-Walled Carbon Nanotubes. *Journal of Nanoscience and Nanotechnology*, 4(8), 995-1004.

[40] Sanchez-Vives, M. V., & Mc Cormick, D. A. (2000). Cellular and network mechanisms of rhythmic recurrent activity in neocortex. *Nat. Neurosci.*, Oct, 3(10), 1027-34.

[41] Cogan, S. F. (2008). Neural Stimulation and Recording Electrodes. *Annu. Rev. Biomed. Eng.*, Aug, 10(1), 275-309.

[42] de Levie, R. (1964). On porous electrodes in electrolyte solutions-IV. *Electrochimica Acta.*, Sep, 9(9), 1231-45.

[43] Lu, Y., Li, T., Zhao, X., Li, M., Cao, Y., Yang, H., et al. (2010). Electrodeposited polypyrrole/carbon nanotubes composite films electrodes for neural interfaces. *Biomaterials.*, Jul, 31(19), 5169-81.

[44] Ben-Jacob, E., & Hanein, Y. (2008). Carbon nanotube micro-electrodes for neuronal interfacing. *Journal of Materials Chemistry*, 18(43), 5181.

[45] Keefer, E. W., Botterman, B. R., Romero, M. I., Rossi, A. F., & Gross, G. W. (2008). Carbon nanotube coating improves neuronal recordings. *Nat Nano.*, Jul, 3(7), 434-9.

[46] Compte, A., Reig, R., Descalzo, V. F., Harvey, MA, Puccini, G. D., & Sanchez-Vives, M. V. Spontaneous High-Frequency (10-80 Hz) Oscillations during Up States in the Cerebral Cortex In Vitro. *J. Neurosci.*, 28(51), 13828-44.

[47] Sanchez-Vives, M. V. (2012). Spontaneous rhythmic activity in the adult cerebral cortex in vitro. *Isolated brain circuits. Ballanyi K. Springer*.

[48] Reig, R., Mattia, M., Compte, A., Belmonte, C., & Sanchez-Vives, M. V. (2010). Temperature modulation of slow and fast cortical rhythms. *J. Neurophysiol.*, Mar, 103(3), 1253-61.

[49] Merrill, E. G., & Ainsworth, A. (1972). Glass-coated platinum-plated tungsten microelectrodes. *Med. & biol. Engng.*, Sep, 10(5), 662-72.

IntechOpen